

A numerical model of sediment-laden turbulent flow in an open channel

Joon-Yong Yoon and Seung-Kyu Kang

Abstract: A numerical analysis of sediment-laden flow is carried out. Velocity and suspended sediment concentration profiles are compared with the experiments in open channel flow. The $k-\omega$ turbulence model is selected for the fully turbulent flow field because this model has shown good results for wall-bounded flows and for flows on rough surfaces. The concentration equation that takes into account the settling velocity is adopted for the concentration field. A new eddy viscosity model is proposed in the turbulence modeled equations to couple the velocity field and the concentration field. The bed load thickness and surface roughness are considered in this study, and reasonable predictions are achieved.

Key words: numerical simulation, suspended sediment transport, open channel flow, $k-\omega$ turbulence model.

Résumé : Une analyse numérique d'un écoulement chargé de sédiments a été effectuée. Les profils de vitesse et de concentration de sédiments en suspension sont comparés aux essais d'écoulement dans un canal à surface libre. Le modèle de turbulence $k-\omega$ est choisi pour le champ de pleine turbulence parce que ce modèle a démontré de bons résultats pour les écoulements limités par des murs et pour les écoulements sur des surfaces rugueuses. L'équation de concentration qui tient compte de la vitesse de sédimentation a été retenue pour le champ de la concentration. Un nouveau modèle de viscosité tourbillonnaire est proposé dans les équations de modélisation de la turbulence afin de jumeler les champs de la vitesse et de la concentration. Dans cette étude, on tient compte de l'épaisseur de la charge de fond et de la rugosité de la surface; on atteint des prédictions raisonnables.

Mots clés : simulation numérique, transport de sédiments en suspension, écoulement dans un canal à surface libre, modèle de turbulence $k-\omega$.

[Traduit par la Rédaction]

1. Introduction

The research on sediment-laden flow is of great interest to river and environmental engineers and earth scientists. We must deal with a two-phase flow of mixed liquid and solid to analyze the transport of suspended sediment in rivers, the transport of grain through a channel, the filtering of suspended particles in industrial water, and sea contamination by particulate sediment. Hence, many researchers have studied sediment-laden flow for several decades.

Rouse (1937), who was one of the earliest researchers of sediment flow, offered an analytical solution of concentration profile in fully developed two-dimensional open channel flow. This concentration profile under ideal conditions has played an important role as a basic reference for many researchers (Woo et al. 1988; Cellino and Graf 1999; Greimann and Holly 2001). Einstein and Chien (1955) pro-

posed a drag law based on the mixing length theory between fluid and sediment. Bechteler and Schimpf (1984) compared velocity profiles and the turbulence diffusion coefficients of several cases. van Rijn (1984) derived a concentration equation in a steady state and suggested a function that takes into account sediment settling velocity and the sediment diffusion coefficient, which directly controls hydraulic parameters for the suspended load. Celik and Rodi (1988, 1991) used a two-dimensional form of the sediment-transport equation and applied the so-called entrainment model to give the flux boundary condition for the concentration equation at some reference level near the bed. They solved the Reynolds-averaged Navier–Stokes equations along with the $k-\varepsilon$ turbulence model and concentration equation. Umeyama and Gerritsen (1992) applied a modified mixing length theory to estimate velocity profile in sediment-laden flow. Recently, Kovacs (1998) considered the roughness effect on the bed and divided a flow field into two layers. In the thin inner flow region, near the bed, a new logarithmic velocity profile that considers a rough wall velocity distribution was derived to replace its clear-water counterpart, which is the logarithmic law of the wall. Here, the concentration was approximated with a power law function. On the other hand, the governing differential equations were solved without any approximations in the outer flow region.

The fluid that is transporting suspended particles is assumed to be decreased in velocity by the fluid–particle interactions (Sundaresan et al. 2003). However, previous

Received 13 August 2003. Revision accepted 25 August 2004. Published on the NRC Research Press Web site at <http://cjce.nrc.ca> on 12 March 2005.

J.-Y. Yoon¹ and S.-K. Kang, Department of Mechanical Engineering, University of Hanyang, Ansan city, Kyunggi-Do 425-791, Korea.

Written discussion of this article is welcomed and will be received by the Editor until 30 June 2005.

¹Corresponding author (e-mail: joyoon@hanyang.ac.kr).

numerical researchers (Bechteler and Schrimpf 1984; Celik and Rodi 1988, 1991; Umeyama and Gerristen 1992; Kovacs 1998) took no account of any fluid-particle interaction. They usually used the wall function approach to predict profiles of mean velocities and turbulence quantities even though this approach assumes application of turbulent flow over smooth wall without pressure gradient in the flow direction (Wilcox 1988). Therefore, it has many defects when all the surface is rough or the pressure gradient is severe, such as flows over complex terrain.

This study proposes a numerical model for the analysis of sediment-laden flow in an open channel. This research adopts the two-equation turbulence model to estimate the velocity field. The selection of a turbulence model is very important because the turbulence model affects the velocity field. We applied the k - ω turbulence model, which was suggested by Wilcox (1988) and has been used by many researchers, especially on the wall-bounded flows. It offers advantages in considering sand-grain roughness on the wall boundary. Since it does not use wall function approach, more grids near the wall are required than the standard k - ϵ model. However, results show much better velocity profiles than the standard k - ϵ model or various low-Reynolds k - ϵ models (Patel and Yoon 1995), and general convection-diffusion equation for the sediment concentration, in which the settling velocity of the particle is considered, is applied. Unlike previous researchers who did not consider the fluid-particle interactions, so-called a drag law, we applied Einstein and Chien's (1955) idea in the turbulence modeled equations to consider this effect. The numerical results were compared with Coleman's (1981, 1986) experimental data. Comparing with other numerical studies that tried to reproduce Coleman's concentration profile, we added the idea of the bed load thickness that may exist in the experiment.

2. Governing equations

2.1. Reynolds-averaged Navier-Stokes equations

The flow and sediment transport models employed here are a steady state, incompressible, and turbulent flow. The Reynolds-averaged equations of continuity and momentum, in non-dimensional form, can be written in Cartesian tensor notation as follows:

Continuity equation

$$[1] \quad \frac{\partial U_i}{\partial x_i} = 0, \quad (i = 1, 2)$$

Momentum equation

$$[2] \quad \rho \frac{\partial U_i}{\partial t} + \rho U_j \frac{\partial U_i}{\partial x_j} = -\frac{\partial P}{\partial x_i} + \frac{\partial}{\partial x_j} (2\mu \mathbf{S}_{ij} - \overline{\rho u'_i u'_j}), \quad (j = 1, 2)$$

The vectors U_i and x_j are mean velocity and position, u'_i is the fluctuating velocity in the x ($i = 1$) and y ($i = 2$) directions, P is the static pressure, t is the time, ρ is the density of fluid, μ is the molecular viscosity, and \mathbf{S}_{ij} is the strain-rate tensor defined by

$$[3] \quad \mathbf{S}_{ij} = \frac{1}{2} \left(\frac{\partial U_i}{\partial x_j} + \frac{\partial U_j}{\partial x_i} \right)$$

where $-\overline{\rho u'_i u'_j}$ is the Reynolds stress tensor. Reynolds stresses are related to the mean rates of strain through eddy viscosity, ν_t , by Boussinesq approximation

$$[4] \quad -\overline{u'_i u'_j} = \nu_t \left(\frac{\partial U_i}{\partial x_j} + \frac{\partial U_j}{\partial x_i} \right) - \frac{2}{3} k \delta_{ij}$$

where $k = \overline{u'_i u'_i} / 2$ is turbulent kinetic energy and δ_{ij} is Kronecker delta.

2.2. Turbulence modeled equations

The velocity field affects the concentration field; therefore, the velocity profile should be calculated very carefully to get the best concentration profile. Previous research often used a log-law profile or a power-law velocity profile to derive the velocity field. Recently, the mixing length theory, which is a zero-equation model, or the k - ϵ turbulence model, which is a two-equation model, has been applied to simulate turbulent velocity profile (Bechteler and Schrimpf 1984; Celik and Rodi 1988, 1991; Umeyama and Gerristen 1992; Kovacs 1998). In this study, we have chosen the two-equation k - ω turbulence model to get the better velocity profile. This model is believed to be proper for sediment-laden flow because it can consider the effects of surface roughness associated with bed load. According to Wilcox (1988), ω is the ratio of turbulence dissipation rate ϵ to the turbulent kinetic energy k and may be regarded as a characteristic time scale of the turbulence. The k - ω model equations are

$$[5] \quad \frac{\partial k}{\partial t} + U_j \frac{\partial k}{\partial x_j} = \tau_{ij} \frac{\partial U_i}{\partial x_j} - \varphi^* k \omega$$

$$+ \frac{\partial}{\partial x_j} \left[(\nu + \sigma^* \nu_t) \frac{\partial k}{\partial x_j} \right]$$

$$[6] \quad \frac{\partial \omega}{\partial t} + U_j \frac{\partial \omega}{\partial x_j} = \alpha \frac{\omega}{k} \tau_{ij} \frac{\partial U_i}{\partial x_j} - \varphi \omega^2$$

$$+ \frac{\partial}{\partial x_j} \left[(\nu + \sigma \nu_t) \frac{\partial \omega}{\partial x_j} \right]$$

where τ_{ij} is the specific Reynolds stress tensor and ν is the kinematic viscosity. The eddy viscosity (ν_t) is given by

$$[7] \quad \nu_t = \gamma^* \frac{k}{\omega}, \quad (\gamma^* = 1.0)$$

The values of the closure coefficients are $\varphi = 3/40$, $\varphi^* = 0.09$, $\alpha = 5/9$, and $\sigma = \sigma^* = 0.5$ (Wilcox 1988). To include the effect of sand-grain roughness (k_s), two different boundary values of ω are used, depending on the value of k_s^+ ($k_s^+ = u_\tau k_s / \nu$). Here, u_τ is the shear velocity. A rough-wall boundary condition for ω is employed as suggested by Wilcox (1988) and proved by Patel and Yoon (1995).

Table 1. Flow conditions for calculation (Coleman 1981, 1986).

Run No.	D_{50} (mm)	Q_s (kg)	Q (m ³ /s)	h (mm)	δ (mm)	\bar{U} (m/s)	C_b ($\times 10^{-3}$)	s	D_h (m)	Re ($\times 10^5$)	w_s (cm/s)
01	—	0	0.064	172	132	1.045	—	—	0.688	7.35	—
02	0.105	0.91	0.064	171	120	1.051	1.39	2.65	0.684	7.93	1.0
09	—	7.27	0.064	172	136	1.045	15.5	2.65	0.688	7.88	1.0
22	0.210	0.91	0.064	170	122	1.058	2.13	2.65	0.680	7.80	2.49
29	—	7.27	0.064	168	130	1.070	57.0	2.65	0.672	7.70	2.49
33	0.420	0.91	0.064	174	128	1.033	0.695	2.65	0.696	7.55	5.70
40	—	7.27	0.064	171	125	1.050	100	2.65	0.684	7.62	5.70

Note: Re, Reynolds number.

$$\begin{aligned}
 [8] \quad \omega &= \frac{2500v}{k_S^2}, & k_S^+ < 25 \\
 \omega &= \frac{100u_\tau}{k_S}, & k_S^+ \geq 25
 \end{aligned}$$

In the computer code the appropriate value is applied depending on the local roughness Reynolds number (k_S^+).

2.3. Concentration equation

Following Yoon (1993), we start from the assumption that the suspended sediment load is supported by turbulent diffusion, with an upward diffusion velocity of particles balanced by their downward fall velocity. From conservation of suspended sediment in a finite control volume, the generalized concentration equation may be written as

$$[9] \quad \gamma \int_V \left(\frac{\partial C}{\partial t} + \nabla \cdot (C\bar{u}_p) - \nabla \cdot (\Gamma_S \cdot \nabla C) \right) dV = 0$$

where C is the concentration of sediment by weight ((weight of sediment)/(weight of water)), γ is specific gravity, Γ_S is eddy diffusivity or diffusion coefficient for suspended sediment, and \bar{u}_p represents the mean velocity vector of the suspended sediment within the control volume. The first term represents the rate of change of sediment within the control volume, the second term represents convection with the mean flow, and the third term represents turbulent transport, modeled by eddy diffusivity. The application of eq. [9] to an elemental control volume leads to the differential transport equation

$$[10] \quad \frac{\partial C}{\partial t} + \nabla \cdot (C\bar{u}_p) = \nabla \cdot (\Gamma_S \cdot \nabla C)$$

Here, we assume $\bar{u}_p = \bar{u}_f + \bar{w}_s$, where \bar{u}_f and \bar{w}_s represent the flow mean velocity and the sediment settling velocity, respectively. If this is applied to an incompressible fluid and the settling velocity is assumed to be constant, such as $\bar{w}_s = -w_s \bar{j}$ (here, \bar{j} is the y -directional vector), the general suspended sediment concentration equation is obtained in the form

$$[11] \quad \frac{\partial C}{\partial t} + U_j \frac{\partial C}{\partial x_j} = \frac{\partial}{\partial x_j} \left(\Gamma_S \frac{\partial C}{\partial x_j} \right)$$

where $U_j = (U, V - w_s)$, U and V are the components of mean velocity in directions x and y , respectively, and w_s is the sediment settling velocity. The concentration equation

introduces an additional unknown Γ_S , which needs to be prescribed. Also, it is necessary to modify the k - ω turbulence model of Wilcox to account for the effect of the suspended sediment of the flow, i.e., on the eddy viscosity ν_t . For the latter, we propose a new eddy viscosity for the k - ω turbulence model that considers the effect of the suspended sediment following the idea of Einstein and Chien (1955). Einstein and Chien used the following mixing length theory when turbulent flow included suspended sediment:

$$[12] \quad \tau_{ij} = \left(1 + \frac{\rho_s - \rho}{\rho} C \right) \rho l^2 \left| \frac{dU}{dy} \right| \frac{dU}{dy}$$

where ρ_s is the density of sediment and l is the turbulent mixing length. According to this, the eddy viscosity in sediment-laden flow is proposed for the turbulence model such as

$$[13] \quad \nu_t = \gamma^* \frac{k}{\omega} \left[1 + \left(1 - \frac{1}{s} \right) C \right]$$

where s ($s = \rho_s/\rho$) is the specific gravity of the sediment. To obtain an expression for the eddy diffusivity Γ_S , the assumption is made as follows:

$$[14] \quad \Gamma_S = \beta \nu_t$$

Here β is the reciprocal of the turbulent Schmidt number (σ_t).

The flow field boundary conditions are given by the no-slip condition at the bed surface with the assumption that fluid velocity is much faster than that of bed load and by assuming no tangential shear stress at the water surface. The Neumann boundary condition for a suspended sediment concentration is prescribed by the no-flux condition at the water surface. The Dirichlet boundary condition is given by a reference suspended concentration (C_b) at the bed of Coleman's experiment (1981, 1986).

3. Experimental data

The results obtained from the model are compared with Coleman's experimental data (1981, 1986). Coleman's experiments were performed in a recirculating flume with a rectangular Plexiglas® channel 356 mm wide and 15 m long, with a slope adjustment capability for maintaining uniform flow. Velocity and concentration profiles were measured at a vertical located on the flume channel centerline and at the position of 12 m downstream from the entrance. First, Coleman measured velocity in clear water and then gradu-

Fig. 1. Non-dimensional velocity profiles (symbols, Coleman’s experiment (1986); lines, present computation): (a) $Q_s = 0.91$ kg and (b) $Q_s = 7.27$ kg.

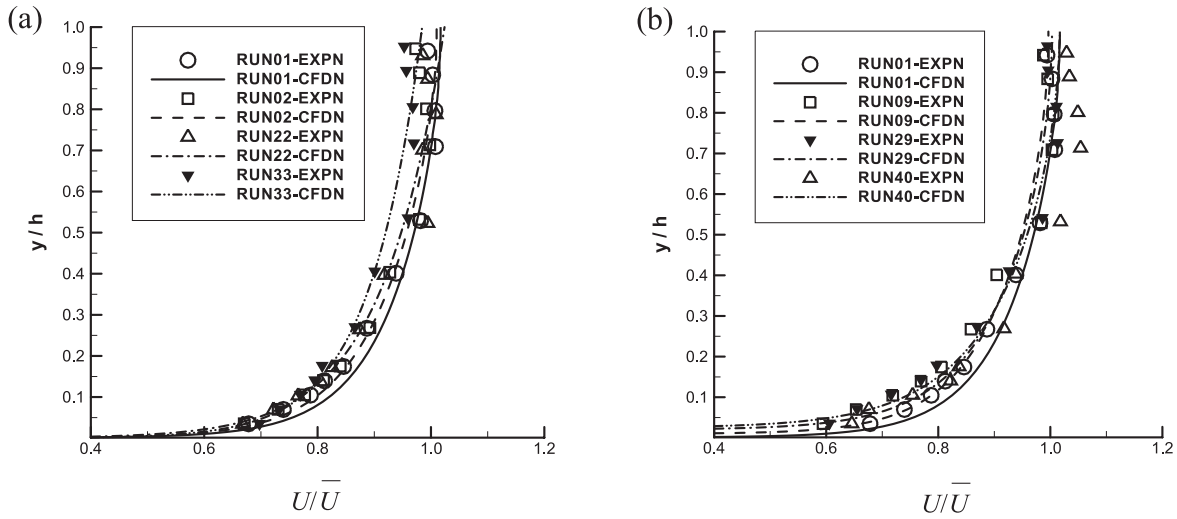


Fig. 2. Concentration and bed load thickness distributions (symbols, Coleman’s experiment (1986); lines, present computation): (a) $D_{50} = 0.105$ mm, (b) $D_{50} = 0.210$ mm, and (c) $D_{50} = 0.420$ mm.

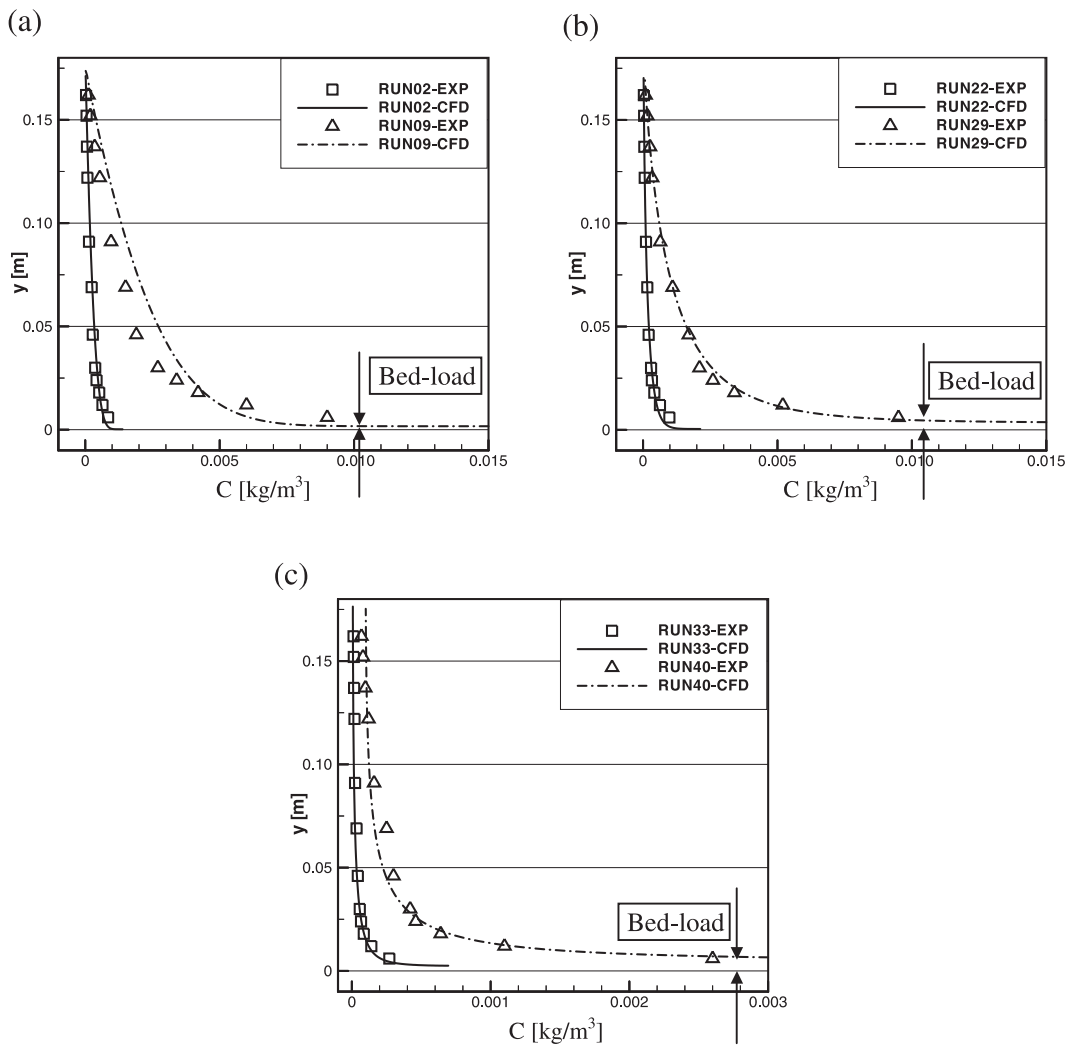
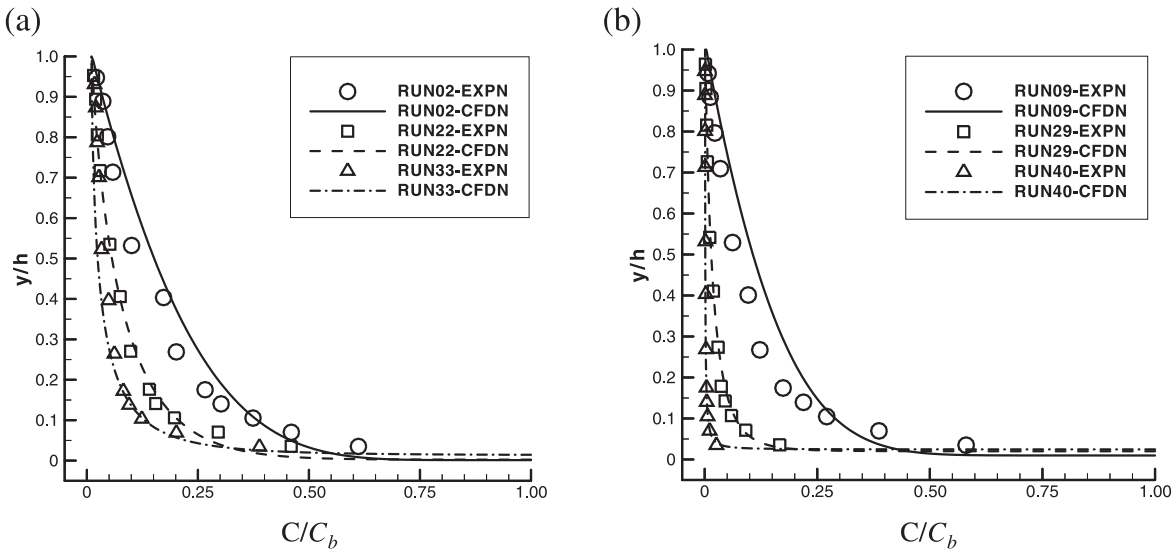


Fig. 3. Nondimensional concentration profiles (symbols, Coleman’s experiment (1986); lines, present computation): (a) $Q_s = 0.91$ kg and (b) $Q_s = 7.27$ kg.



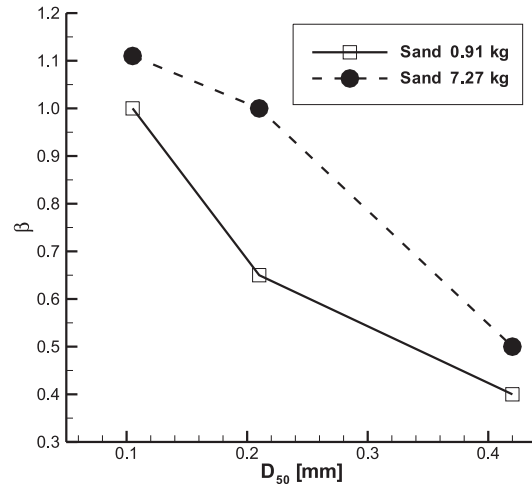
ally added sediment. He measured the changes in the velocity field and in the sediment concentration distribution in the flow. Flow depths (h) varied between 16.8 and 17.4 cm, and the channel width, W , is 35.6 cm, giving an aspect ratio of around 2.

The sediment and flow characteristics are given in Table 1. For all experiments, the discharge Q is held constant at $0.064 \text{ m}^3/\text{s}$, corresponding to $q = Q/W = 0.1798 \text{ m}^2/\text{s}$ discharge per unit width. Reynolds numbers based on the average of flow velocity (\bar{U}) and hydraulic diameter (D_h) have 10^5 order in all cases. Therefore, all flows in this study are judged to be fully turbulent and are much larger than the critical value of the Reynolds number (2000) at which transition to turbulence in an open channel occurs (Schlichting 1979). The settling velocity of suspended sediment is determined from the sphere diameter-settling velocity curve suggested by Rouse (1937), assuming that the sand-grains are spherical. The water density, ρ , is 1000 kg/m^3 . The sediment is sand with a density of ρ_s equal to 2650 kg/m^3 .

4. Numerical scheme

The numerical model employed here is based on the one developed by Patel and Yoon (1995), Yoon and Patel (1996), and Yoon et al. (1996). In this model, the Reynolds-averaged Navier–Stokes equations for an incompressible fluid are solved in a generalized non-orthogonal coordinate system that is generated numerically by the solution of two Poisson equations and by full transformation (Thompson et al. 1985). Here, this study used the SIMPLER algorithm of Patankar (1980) to correct for the pressure and velocities. Governing equations are discretized by the finite analytic method (Chen and Chen 1982). The basic idea of the finite analytic method is to use the local analytic solution in the discrete computational element to obtain the algebraic representation of the governing differential equation. The finite analytic method differs from conventional numerical methods in that it does not directly tamper with the differentials or the derivatives of the governing equation, nor does it need the shape function,

Fig. 4. The profiles of β according to the quantity of sediment (Q_s) and the particle size (D_{50}).



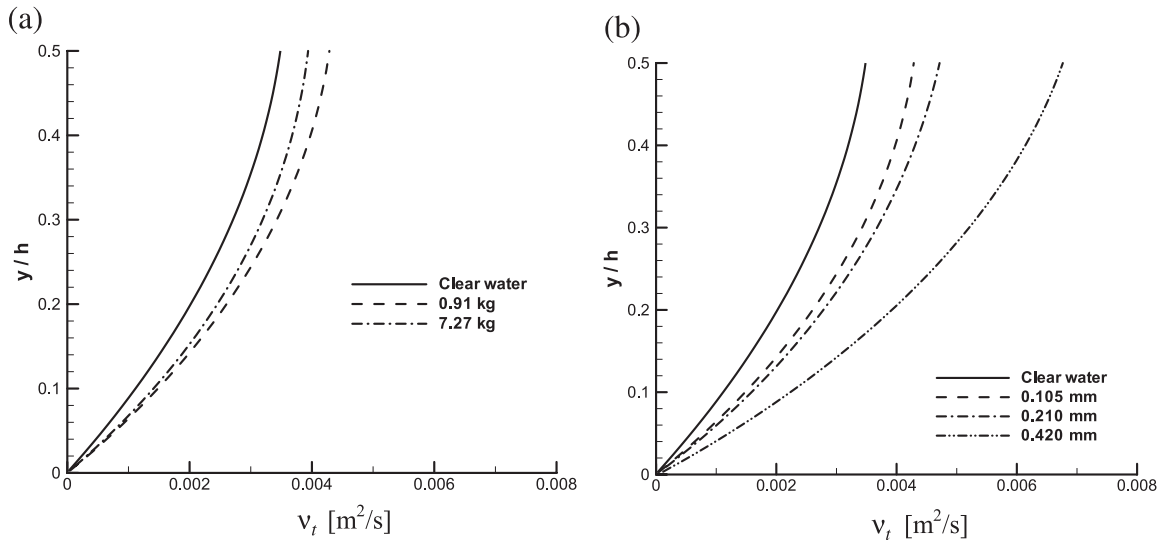
which is made to satisfy the integral form of the governing equation.

5. Results

5.1. Flow field

Figure 1 compares modeled and measured velocity profiles at the sediment quantities (Q_s) of 0.91 and 7.27 kg. The plots are for selected profiles in clear water, as well as those obtained with sediment of size corresponding to D_{50} of 0.105, 0.210, and 0.420 mm, respectively. Figure 1 shows that in sediment-laden flows local velocities near the bed are reduced relative to the equivalent clear-water flow. In the near-bed region, the sediment concentration is very high and eddy viscosity is increased when compared with clear water flow. These figures show that the presence of suspended sediment causes a general reduction of mean flow velocity and that the magnitude of this velocity reduction is positively related to the sediment size. In a free surface region, velocity

Fig. 5. Comparison of eddy viscosity profiles near the bed for (a) different sediment loads with $D_{50} = 0.105$ mm and (b) different grain sizes with $Q_s = 0.91$ kg.



profiles show little difference between the measured and computed values. Our simulation is performed with the assumption of a fully developed two-dimensional flow that shows a negligible effect of secondary flow. However, Coleman's (1981, 1986) experimental flume has a 2.1 aspect ratio. Fully developed flow conditions and the level of secondary current in this flume were documented in experiments by Muste and Patel (1998). Based on these findings, the high aspect ratios that are not <7 must be guaranteed to be exact two-dimensional flow. It is clear that Coleman's experiments are not sufficient to be free of any secondary flow. Therefore, these differences of velocity profiles between the measured and computed values near the free surface are presumed by the secondary flow effect of side walls.

5.2. Concentration field

While conventional numerical analyses related to Coleman's (1981, 1986) sediment-laden flow have ignored the effect of bed load thickness, this study is performed by considering its effect, as it may vary with the amount of sediment. The thickness of the bed load is very important because it affects the computation domain. There is no accurate theory concerning the thickness of the bed load, but Einstein (1950) suggested that thickness of bed load is 1–2 times as large as the particle size in cases where particle size is fine and shear force is small. Engelund (1981) and Wilson (1988) suggested that thickness increases to several times the particle size as the shear force increases. In this application, the average concentration is accurately predicted when the thickness of the bed load varies between 2 and 6 times the sediment size in a 0.91-kg sand mass and between 10 and 16 times in a 7.27-kg sand mass.

Figure 2 shows the prescribed bed load thickness that fits best the experimental data. The thickness of the bed load is negligible in very small quantity of sediment, such as Runs 02, 22, and 33, but it is found to be considerably larger in a quantity of sediment, such as Runs 09, 29, and 40. Thickness increases as a function of the diameter of sediment.

This means that increasing sediment quantity or size can exert great influence upon the flow field. Our numerical approaches predict reasonable concentration profiles in general. However, in the case of Run09 in Fig. 2a, which is the smallest particle size and larger sediment quantity, the difference between the measured and predicted values is largest. The simulated values are over-predicted in the large part of domain and under-predicted near the bed. However, the maximum error is limited to approximately 20% at most.

Figures 3a and 3b compare concentration distributions with variable sizes of particle under the same amount of sediment (Q_s). An examination of the concentration distributions shows that the larger the sediment size, the greater the slope. This means that sediment size and concentration distribution are correlated. The slope is controlled by the magnitude of the turbulent Schmidt number (σ_t). Jobson and Sayre (1970) have proposed σ_t as 1.0 through experimentation, but Karim (1981) and Celik (1983) proposed σ_t as 0.5–1.0. On the other hand, van Rijn (1984) proposed the following empirical formula, assuming β ($1/\sigma_t$) is related to the ratio of settling (w_s) to shear velocity (u_τ):

$$[15] \quad \beta = 1 + 2 \left[\frac{w_s}{u_\tau} \right]^2$$

From a numerical point of view, this value must be prescribed from eqs. [11] and [14]. However, there does not exist a consensus on this value. Hence, arbitrary values are often used for numerical predictions. Celik and Rodi (1988) assumed that σ_t is 1.0 for developing flow in the entrance region of the open channel and is 0.5 in the fully developed region of the flow from their simulation results. Galland et al. (1997), using a Reynolds stress model, achieved good results when the turbulent Schmidt number is 0.7 ($\beta = 1.4$). Most of foregoing research insisted that σ_t had a value <1.0 . That is to say, they agreed that β is larger than 1.0. Recently, however, Cellino and Graf (1999) obtained a β value of <1.0 from their experiments. In this study, good predictions are

obtained when β is 1.0, 1.11, 0.65, 1.0, 0.4, and 0.5 in each case of Runs 02, 09, 22, 29, 33, and 40, respectively.

A suspended sediment transport is affected by the sediment shape, size, and concentration (Vanoni 1977). It is also affected by particle–particle interaction and particle inertia (Greimann and Holly 2001). In this research, we focus on the effect of the sediment size and concentration. Figure 4 shows the variation of β according to the particle size (D_{50}) and the amount of sediment (Q_s), which is the total sediment discharge of the flow. This shows that β is related to the sediment quantity and size. With higher sediment quantity, β increases; with larger sediment size, β decreases. According to eq. [14], the increasing of β , as sediment quantity grows, results in the increasing of the eddy diffusivity. On the other hand, the decreasing β value, as sediment size grows, results in the increasing of the eddy viscosity. It is likely that when the amount of sediment is large, namely when the concentration is increased, the diffusion of sediment is relatively more active, and as sediment size increases, the eddy viscosity is increased. It means that the turbulence length scale is also increased with the size of suspended sediment.

Figure 5 shows profiles of the calculated eddy viscosity in the vicinity of the bed. Figure 5a compares the eddy viscosity profiles for different amounts of sand, and Fig. 5b compares the profiles derived as sediment size is varied. In Fig. 5a the absolute value of the eddy viscosity for sediment-laden flow is bigger than that of the clear water. As the amount of sand is increased, however, eddy viscosity is decreased. This result can be explained as follows. On the basis of Prandtl's mixing length theory, eddy viscosity is defined as (Schlichting 1979)

$$[16] \quad v_t = l^2 \left| \frac{dU}{dy} \right|$$

Here, as the amount of sand increases, the velocity gradient decreases near the bed. This in turn entrains a decrease in eddy viscosity. It seems that flow and suspended sediment interaction in the proposed model is affected. On the other hand, as sediment size increases, the value of eddy viscosity is continuously increased with the increase of the mixing length from eq. [16].

6. Summary and conclusions

In this research, a numerical analysis of sediment-laden flow is carried out. Velocity and suspended sediment concentration profiles are compared with the experiments of Coleman (1981, 1986), which included several cases of varying sediment size and quantity in open channel flow. The k - ω turbulence model is selected for the fully turbulent flow field. The concentration equation, which takes into account the settling velocity, is adopted for the concentration field. In this study the following conclusions are obtained:

- (1) A new eddy viscosity model for the k - ω turbulence model is proposed to couple the velocity field and the concentration field. The interaction between the fluid flow and the suspended sediment is successfully reproduced through this model. Through the numerical approach, β is found to vary with sediment size and concentration.

- (2) A numerical simulation is carried out considering the thickness of the bed load, especially the effects of size and quantity for sand particles.
- (3) Satisfactory predictions for the mean velocity and the sediment concentration profiles are obtained by using the k - ω turbulence model including the effect of sand-grain roughness on the bed.

References

- Bechteler, W., and Schrimpf, W. 1984. Improved numerical model for sedimentation. *ASCE Journal of Hydraulic Engineering*, **110**(3): 234–246.
- Celik, I. 1983. Numerical modelling of sediment transport in open channel flows. *In Mechanics of sediment transport. Edited by B. Mutlu Sumer and A. Müller. A.A. Balkema, Rotterdam, The Netherlands. pp. 173–181.*
- Celik, I., and Rodi, W. 1988. Modeling suspended sediment transport in nonequilibrium situations. *ASCE Journal of Hydraulic Engineering*, **114**(10): 1157–1190.
- Celik, I., and Rodi, W. 1991. Suspended sediment-transport capacity for open channel flow. *ASCE Journal of Hydraulic Engineering*, **117**(2): 191–204.
- Cellino, M., and Graf, W.H. 1999. Sediment-laden flow in open channels under noncapacity and capacity conditions. *ASCE Journal of Hydraulic Engineering*, **125**(5): 455–462.
- Chen, C.-J., and Chen, H.-C. 1982. The finite analytic method. Iowa Institute of Hydraulic Research, The University of Iowa, Iowa City, Iowa. IIHR Report 232-IV.
- Coleman, N.L. 1981. Velocity profiles with suspended sediment. *Journal of Hydraulic Research*, **19**(3): 211–229.
- Coleman, N.L. 1986. Effects of suspended sediment on the open channel velocity distribution. *Water Resources Research*, **22**(10): 1377–1384.
- Einstein, H.A. 1950. The bed-load function for sediment transportation in open channel flows. Department of Agriculture, Washington, D.C. Technical Bulletin 1026.
- Einstein, H.A., and Chien, N. 1955. Effects of heavy sediment concentration near the beds on velocity and sediment distribution. Engineering Division, Missouri River, U.S. Army Corps of Engineers Omaha, Neb. MRD series no. 8.
- Engelund, F. 1981. Transport of bed-load at high shear stress. Institute of Hydrodynamic and Hydraulic Engineering, ISVA, Technical University of Denmark, Lyngby. Progress report 53. pp. 31–35.
- Galland, J.-C., Laurence, D., and Teisson, C. 1997. Simulating turbulent vertical exchange of mud with a Reynolds stress model. Proceedings of the 4th Nearshore and Estuarine Cohesive Sediment Transport Conference, INTERCOH '94, Wallingford, England, 11–15 July 1994. Edited by N. Burt, R. Parker and J. Watts. John Wiley, Toronto. pp. 439–448.
- Greimann, B.P., and Holly, F.M., Jr. 2001. Two-phase flow analysis of concentration profiles. *ASCE Journal of Hydraulic Engineering*, **127**(9): 753–762.
- Jobson, H.E., and Sayre, W.W. 1970. Vertical transfer in open channel flow. *ASCE Journal of Hydraulic Engineering*, **96**(3): 703–724.
- Karim, M.F. 1981. Computer-based predictors for sediment discharge and friction factor of alluvial streams. Ph.D. thesis, University of Iowa, Iowa City, Iowa.
- Kovacs, A.E. 1998. Prandtl's mixing length concept modified for equilibrium sediment-laden flows. *ASCE Journal of Hydraulic Engineering*, **124**(8): 803–812.

- Muste, M., and Patel, V.C. 1998. Velocity profiles for particles and liquid in open channel flow with suspended sediment. *ASCE Journal of Hydraulic Engineering*, **123**(9): 742–751.
- Patankar, S.V. 1980. Numerical heat transfer and fluid flow. Hemisphere Publishing Corporation, Washington, D.C.
- Patel, V.C., and Yoon, J.Y. 1995. Application of turbulence models to separated flow over rough surfaces. *ASME Journal of Fluids Engineering*, **117**: 234–241.
- Rouse, H. 1937. Modern conceptions of the mechanics of fluid turbulence. Transactions, ASCE, **102**: 463–543.
- Schlichting, H. 1979. Boundary-layer theory. 7th ed. McGraw-Hill, New York.
- Sundaresan, S., Eaton, J., Koch, D.L., and Ottino, J.M. 2003. Appendix 2: Report of study group on disperse flow. *International Journal of Multiphase Flow*, **29**(7): 1069–1087.
- Thompson, J.F., Warsi, Z.U.A., and Mastin, C.W. 1985. Numerical grid generation. Elsevier Science Publishing Co., New York.
- Umeyama, M., and Gerritsen, F. 1992. Velocity distribution in uniform sediment-laden flows. *ASCE Journal of Hydraulic Engineering*, **118**(2): 229–245.
- van Rijn, L.C. 1984. Sediment transport. Part II: Suspended load transport. *ASCE Journal of Hydraulic Engineering*, **110**(11): 1613–1641.
- Vanoni, V.A. 1977. Sedimentation engineering. American Society of Civil Engineers, New York.
- Wilcox, D.C. 1988. Reassessment of the scale determining equation for advanced turbulence models. *AIAA Journal*, **26**(11): 1299–1310.
- Wilson, K.C. 1988. Frictional behaviour of sheet flow. Institute of Hydrodynamic and Hydraulic Engineering, Technical University of Denmark, Lyngby. Progress report 67. pp. 11–22.
- Woo, H.S., Julien, P.Y., and Reardon, E.V. 1988. Suspension of large concentrations of sands. *ASCE Journal of Hydraulic Engineering*, **114**(8): 888–898.
- Yoon, J.Y. 1993. Numerical analysis of flow in channels with sand dunes and ice covers. Ph.D. thesis, University of Iowa, Iowa City, Iowa.
- Yoon, J.Y., and Patel, V.C. 1996. Numerical model of turbulent flow over sand dune. *ASCE Journal of Hydraulic Engineering*, **122**(1): 10–17.
- Yoon, J.Y., Patel, V.C., and Ettema, R. 1996. Numerical model of flow in ice-covered channel. *ASCE Journal of Hydraulic Engineering*, **122**(1): 19–26.

List of symbols

- C concentration of sediment by weight
 C_b reference concentration at the bed

- D_{50} sediment size for which 50% of the sediment by weight is finer
 D_h hydraulic diameter
 h channel height
 k turbulent kinetic energy
 k_S equivalent sand-grain roughness,
 k_S^+ local roughness Reynolds number
 l turbulent mixing length
 P static pressure
 Q total volume flow rate
 Q_s total sediment discharge of the flow
 \bar{U} average of flow velocity
 U_i, U_j mean velocity components in directions x_i, x_j
 u_i' fluctuating velocity component in x_i direction
 u_j' fluctuating velocity component in x_j direction
 \bar{u}_f flow mean velocity vector
 \bar{u}_p sediment mean velocity vector
 u_τ shear velocity
 w_S sediment settling velocity
 S_{ij} mean strain rate
 s specific gravity of sand-grain
 t time
 x_i Cartesian coordinates x, y ($i = 1, 2$)
 x_j Cartesian coordinates x, y ($j = 1, 2$)
 U, V mean velocity components in directions x, y
 W channel width
 $\alpha, \varphi, \varphi^*, \gamma^*, \sigma, \sigma^*$ coefficients in k - ω turbulence model
 β correlation coefficient
 γ specific gravity
 δ boundary layer thickness
 δ_{ij} Kronecker delta
 μ molecular viscosity of fluid
 ν kinematic viscosity
 ν_t kinematic eddy viscosity
 ρ fluid density
 ρ_S density of sediment
 σ_t turbulent Schmidt number
 τ_{ij} specific Reynolds stress tensor
 Γ_S eddy diffusivity
 ω specific dissipation rate